

ON THE SIZE OF LEFT-HANDED MATERIAL LENS FOR NEAR-FIELD TARGET DETECTION BY FOCUS SCANNING

G. Wang, Y. Gong, and H. Wang

Department of Telecommunication Engineering
Jiangsu University
301 Xuefu Road, Zhenjiang 212013, China

Abstract—Two focus-scanning schemes, viz. lens-fixed scanning scheme and lens-combined scheme, are proposed for near-field target detection and imaging. Specific lens size must be determined for future lens building in order to achieve desired imaging resolution and convenient data acquisition. Influence of LHM lens size on the performance of two different focus-scanning schemes are investigated and compared by simulating the detection of a perfect electric conductor target of diameter of 2 mm. Numerical simulations indicate that the lens-combined scanning system using thick LHM lens of thickness of two wavelengths requires at least a length of one wavelength to achieve resolution better than 0.4 wavelengths, while the lens-fixed scanning system requires a lens of length of approximately 3 wavelengths. When a thin LHM lens is used, high imaging resolution is not a consequent result for the focus-scanning approaches, although thin lens generally yields high focusing resolution. Some guidelines on the selection of length and thickness of flat LHM lens are reported.

1. INTRODUCTION

Veselago's left-handed materials (LHM) [1] have drawn particular attentions in near-field target detection and imaging [2–4]. Sub-wavelength focusing resolution of flat LHM slab lens beating the diffraction limit has been demonstrated by both theoretical/numerical analysis [5–10] and microwave experiments [11–15], high focusing resolution generally yields high imaging resolution in near-field target and detection. Different from the focusing of convex lens of right-handed material (RHM) or elliptical reflector of perfect electric

conductor (PEC), the focusing of flat LHM lens allows to build a focus-flexible system. The position of the focal point of flat LHM slab lens can be adjusted in both the lateral and depth directions by moving the point source.

Recently, a focus-scanning approach for near-field target detection and imaging by using flat LHM lens was proposed [16]. As shown in Fig. 1, when the probe is moved on one side of flat lens according to designated scanning grids, the focal point can be scanned on the other side of the flat lens. After recording and calculating the backscattered microwave field level, near-field target imaging can be implemented by screening the field level at each scanning point on the grids. The proposed approach is demonstrated to provide imaging resolution higher than the focusing resolution of flat LHM lens [16], significant enhancement of the backscattered microwave [17], convenient data acquisition, and potential of real-time screening, which make the proposed approach highly desirable for near-field small target detection and imaging.

However, achieving the subwavelength imaging is not a straightforward result by using LHM lens of arbitrary sizes. In practice, there may also be restrictions on the size of lens from the target detection scenario. As a result, the size or even the shape of LHM lens must be designed. Several lens factors may affect the focusing of flat LHM lens and thus the imaging resolution of the proposed focus-scanning scheme for target detection. Detailed study of such factors will be helpful to future lens design. In [16], effects of material losses of LHM lens have been discussed. In [17], effects of lens refraction index mismatch were investigated. In these studies, the LHM lens are supposed to be long enough, and of fixed thickness of two wavelengths. In [18] and [19], the effects of lens thickness and size on the focusing properties of flat LHM lens have been studied analytically and numerically. In [20], experimental observation of lens size on the focusing of flat LHM lens has been reported. But the focusing properties could not characterize the scanning performance of our scheme proposed for target detection and imaging, although there is some underlying relation between them [16].

For near-field target detection and imaging, proper flat LHM lens should be used. The imaging schemes proposed in [16] were implemented by using long or infinite-extended flat LHM slab. For application such as early breast tumor detection, short LHM lens may be required. Specific sizes such as length and thickness of LHM lens in the focus-scanning system are to be determined. Moreover, we may combine the antenna probe and a LHM lens of certain specific size together to form a lens-combined LHM probe. The antenna probe

behind the LHM lens can be automatically adjusted backwards and forwards to scan the focal point in depth direction. The combined LHM probe can be moved along the surface of region under detection to scan the focal point in lateral direction. The lens-combined probe will take lens size small as possible so that convenient data acquisition such as with the ultrasonic probe can be implemented.

In this paper, we will investigate the influence of LHM lens thickness and length on the performance of the proposed schemes. For demonstration, the detection and imaging of a PEC target of diameter of 2 mm behind the flat LHM lens will be simulated by two-dimensional finite-difference time-domain (FDTD) method. In Section 2, effects of lens size on the resolution of lens-fixed scanning scheme are studied. In Section 3, lens-combined focus-scanning approach is proposed, and the effects of lens size on its performance are investigated. In Section 4, comparison between the lens-fixed and lens-combined imaging schemes for target detection are reported, and some guidance in the selection of LHM lens is provided.

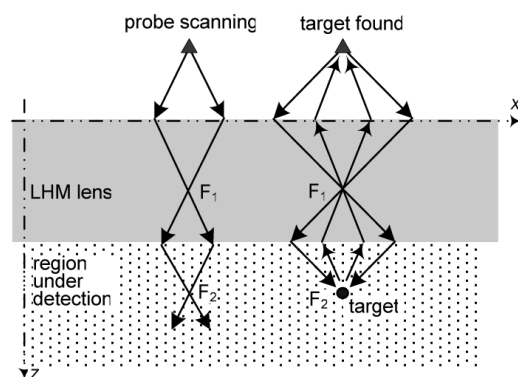


Figure 1. Target detection and imaging by using flat LHM lens and scanning the focal point.

2. LHM LENS FOR LENS-FIXED SCANNING SYSTEM

The focus-scanning scheme for target detection with flat LHM lens can be implemented in different ways. The approach proposed in [16], referred to as lens-fixed scanning scheme, keeps the flat LHM lens stationary on the surface of region under detection when the antenna probe is scanned. The lens-fixed scheme is shown in Fig. 2. By moving the antenna probe in front of the flat LHM lens according to

designated scanning grids, the focal point can be scanned in region under detection behind the flat LHM lens. After recording and calibrating the backscattered microwave field level, imaging of the region under detection can be conducted by screening the field level at each scanning point on the grids. Therefore, almost real-time near-field target imaging can be performed.

In practice, the lens-fixed scanning scheme requires long LHM lens of size quite larger than the region under detection. The performance of lens-fixed scanning has been investigated in detail in [16], where the lens is fixed to have thickness of $d = 2\lambda$ to guarantee enough detection depth. But it is still unclear whether or not other lens thickness can be used to obtain better scanning resolution.

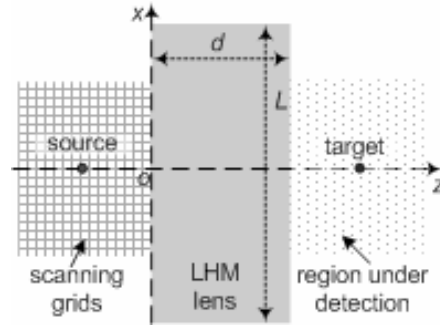


Figure 2. Target detection and imaging by lens-fixed scanning system.

Generally, the use of a thin flat LHM lens in a focusing system will improve the focusing resolution due to the surface plasmons effects excited by the evanescent components of the incident field [18]. But for target detection shown in Fig. 2, it is not always the case. For thin LHM lens, the focal point on image plane predicted by Snell's Law is in the vicinity of LHM lens surface. When a PEC target is set at the focal point, the plasmons effects on the lens surface may suffer more influence from the target. During the scanning, the nearby plasmons will also affect the detection. As a result, the imaging resolution of target detection by using thin LHM lens in lens-fixed system shown in Fig. 2 may be not as high as desired.

For demonstration, we consider a flat LHM lens of length of 20λ . In our FDTD simulations, we follow the definitions as used in [16]. The microwave used for detection is 10 GHz, and the LHM lens is set to have $\epsilon_r = \mu_r \approx -1 - 0.006i$ and thus refraction index $n \approx -1 - 0.006i$ as defined in [16]. The imaginary part $0.006i$ defines very weak LHM losses. LHM losses of the same order as in the

LHM of Eleftheriades' experiment [13] can also be considered. Other simulation considerations including the definition of LHM lens, the use of transition layer between LHM and vacuum, and the perfectly matched layer in our FDTD codes are described in [16].

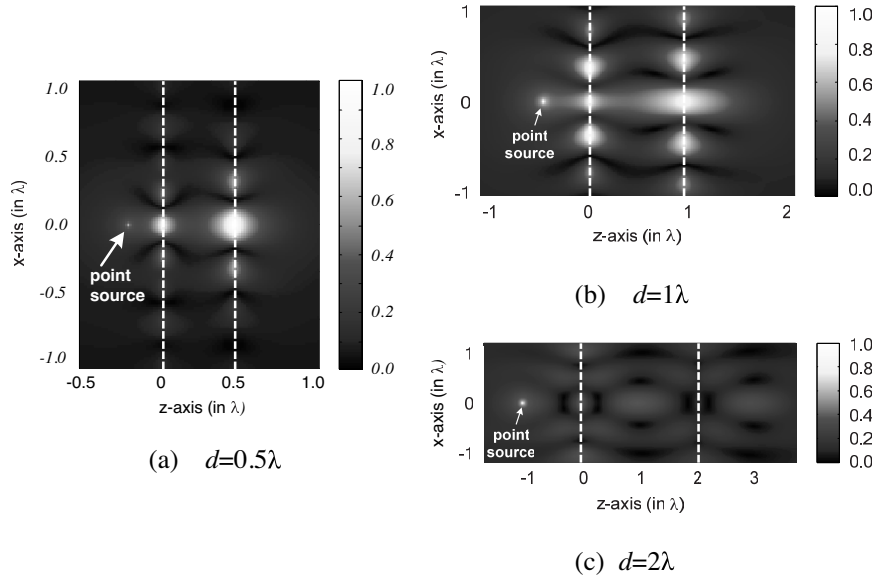


Figure 3. Focusing of microwave by LHM lenses (local) of length 20λ and different thickness.

Figure 3 shows the focusing of flat LHM lens of different thickness. For lens of thickness of $d = 0.5\lambda$, no unambiguous focusing spot outside the lens can be detected on the image plane in Fig. 3(a) as predicted in theory due to the strong surface plasmons. For lens of thickness of $d = 2\lambda$, clear focusing spot outside the lens can be detected on the image plane, as shown in Fig. 3(c). For lens of thickness of $d = 1\lambda$, plasmons on lens surface and the focusing spot outside the lens tend to be separated so that the bright spot is elongated, as shown in Fig. 3(b). Fig. 4 shows the lateral beam profiles of the focused microwave by LHM lens of different thickness, from which the lateral focusing resolution can be measured to be approximately 0.25λ , 0.30λ and 0.36λ for lenses of $d = 0.5\lambda$, $d = 1.0\lambda$ and $d = 2.0\lambda$, respectively. It is observed that thinner lens provides better focusing resolution as expected.

When a PEC target of diameter of 2 mm is set at the predicted focal point of flat LHM lens, image of the 2-mm target can be reconstructed according to the focus scanning scheme as shown in Fig. 2. Fig. 5 shows the lateral beam profiles extracted at the target

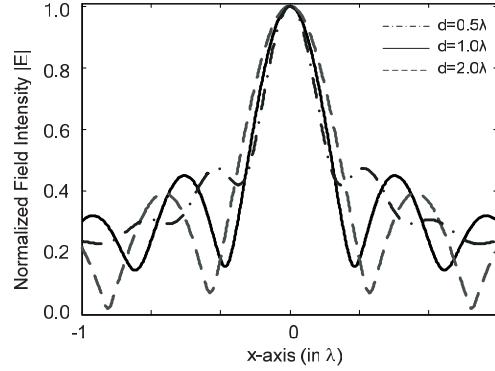


Figure 4. Lateral beam profiles of focused microwave on the image plane.

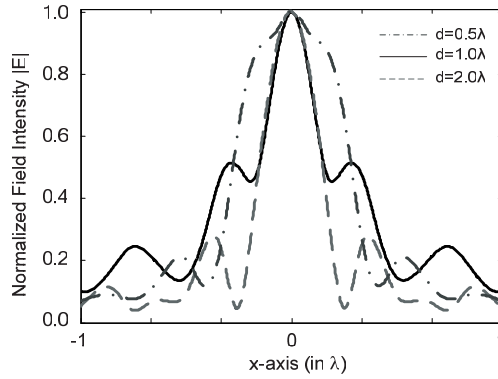


Figure 5. Lateral beam profiles extracted at target position on the reconstructed images obtained by focus-scanning scheme with LHM lens of different thickness.

position on the image reconstructed, from which the lateral imaging resolution of the lens-fixed scanning scheme can be measured to be approximately 0.47λ , 0.21λ and 0.23λ for lenses of thickness $d = 0.5\lambda$, $d = 1.0\lambda$ and $d = 2.0\lambda$, respectively.

We have the observation that by using thin LHM lens of $d = 0.5\lambda$, one acquires the best focusing resolution among the three scenarios, but the worst imaging resolution in lens-fixed focus-scanning imaging. Therefore, the size of LHM lens should be properly selected in future LHM lens design for lens-fixed scanning scheme.

3. LHM LENS FOR LENS-COMBINED SCANNING SYSTEM

Another way to carry out the proposed focus-scanning scheme is to combine the probe antenna and LHM lens of moderate size together, so that an LHM lens-combined probe is formed, as shown in Fig. 6. The focus-scanning with such a probe will be referred to as lens-combined scanning.

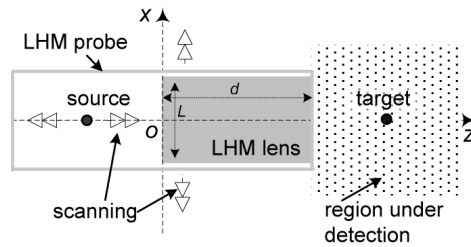


Figure 6. Target detection and imaging by lens-combined scanning system.

In the lens-combined scanning system, one may move the lens-combined probe according to designated grids along the surface of region under detection to scan the focal point in lateral direction. At each scanning point in the grids, the probe antenna behind the lens is automatically adjusted backwards and forwards to scan the focal point in depth direction. Different from the lens in the lens-fixed scanning system, the size of lens in the combined probe should be moderate.

Obviously, there are two parameters need to be determined in the LHM lens-combined probe design. One is the lens thickness d , the other is the lens size L , as marked in Fig. 6. The influence of thickness d and length L will be investigated by simulating the detection and imaging of the 2-mm PEC target.

Figure 7 shows the lateral beam profiles extracted at target position on the image reconstructed by scanning the combined probe of LHM lens of thickness $d = 0.5\lambda$ and different L . The lateral imaging resolutions for probe of lens $L = 0.5\lambda$, $L = 1.0\lambda$, $L = 1.5\lambda$ and $L = 2.0\lambda$ are measured to be approximately 0.36λ , 0.22λ , 0.51λ and 0.45λ , respectively. We have the observation that for the lens-combined scanning, probe with lens of thickness $d = 0.5\lambda$ works, and probe with lens of $L = 1.0\lambda$ provides the highest resolution (0.22λ) among the four. This may be attributed to the fact that probe with lens of $L = 1.0\lambda$ has distinct surface plasmons so that the 2-mm PEC target at $0.25d$

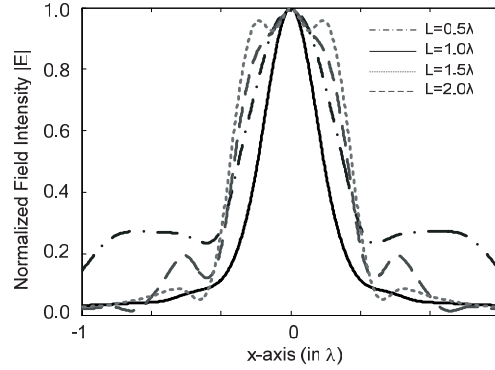


Figure 7. Lateral beam profiles extracted at target position on the image reconstructed by the lens-combined scanning with lens of $d = 0.5\lambda$ and different L .

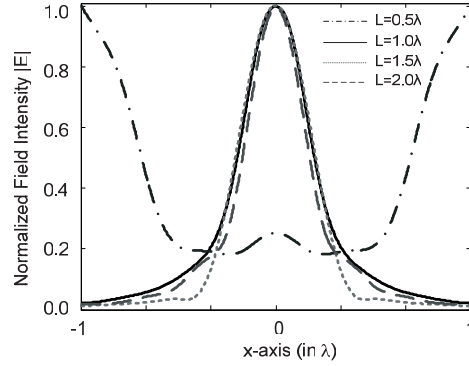


Figure 8. Lateral beam profiles extracted at target position on the image reconstructed by the lens-combined scanning with lens of $d = 1.0\lambda$ and different L .

away from the lens surface has little impacts on the focus-scanning detection.

Figure 8 shows the lateral beam profiles extracted at target position on the image reconstructed by scanning the combined probe of LHM lens of thickness $d = 1.0\lambda$ and different L . The lateral imaging resolutions for probe of lens $L = 1.0\lambda$, $L = 1.5\lambda$ and $L = 2.0\lambda$ are measured to be approximately 0.28λ , 0.30λ and 0.25λ , respectively. But the lateral imaging resolutions for proper lens $L = 0.5\lambda$ is not measured because the narrow lens ($d/L = 2$) focuses/refocuses so little microwave that the field level is much less than those transported by

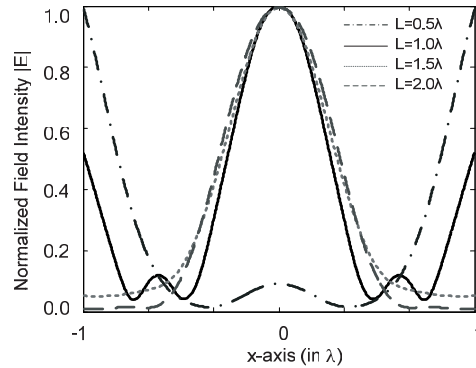


Figure 9. Lateral beam profiles extracted at target position on the image reconstructed by the lens-combined scanning with lens of $d = 2.0\lambda$ and different L .

other mechanism such as diffraction.

Figure 9 shows the lateral beam profiles extracted at target position on the image reconstructed by scanning the combined probe of LHM lens of thickness $d = 2.0\lambda$ and different L . The lateral imaging resolutions for probe of lens $L = 1.0\lambda$, $L = 1.5\lambda$ and $L = 2.0\lambda$ are measured to be approximately 0.38λ , 0.43λ and 0.46λ , respectively. Similar to that in Fig. 8, the lateral imaging resolutions of probe scanning with lens of $L = 0.5\lambda$ is not measured. We have the observation that the corresponding field level is lower than that in Fig. 8 due to the use of a narrower lens ($d/L = 4$ here).

It should be remarked that although the probe with lens of $L = 1.0\lambda$ in Fig. 9 has the same shape factor ($d/L = 2$) as the probe with lens of $L = 0.5\lambda$ in Fig. 8, the lens of $L = 1.0\lambda$ provides better focusing than the lens of $L = 0.5\lambda$ so that a resolution is measured. Anyway, the probe with lens $L = 1.0\lambda$ in Fig. 9 is relatively narrower in shape than the probe with lens $L = 1.0\lambda$ in Fig. 8, thus the scanning suffers more influence of the edge of its narrow shape, which can be observed by comparing the two solid curves in Fig. 8 and Fig. 9.

The resolutions shown in Figs. 7, 8 and 9 are listed in Table 1. It is observed that for the lens-combined scanning, $L = 1.0\lambda$ seems to be a suitable length for probe lens.

4. FURTHER DISCUSSION

Several observations should be further discussed for better understanding the lens-fixed and lens-combined focus-scanning scheme.

Table 1. Imaging resolutions for scanning with probe of different lens.

Resolution (in λ)	$L = 0.5\lambda$	$L = 1\lambda$	$L = 1.5\lambda$	$L = 2\lambda$
$d = 0.5\lambda$	0.36	0.22	0.51	0.45
$d = 1\lambda$	–	0.28	0.3	0.25
$d = 2\lambda$	–	0.38	0.43	0.46

4.1. Thin or Thick LHM Lens

It is generally accepted that better focusing will lead to higher scanning resolution because better focusing implies smaller foot-print of the focused beam. But our simulations with thin lens of $d = 0.5\lambda$ and $L = 20\lambda$ for lens-fixed scanning shows high focusing resolution (0.25λ) but low imaging resolution (0.47λ).

To reveal the underlying physics, we study the refocusing of microwave backscattered from the PEC cylinder located at the center of the image plane ($d/2$ away behind the lens). Fig. 10(a) shows the refocusing of backscattered microwave, Fig. 10(b) shows the electric field level distributed along the surface of lens. We have the observation that the refocusing on the source plane suffers more from the nearby surface plasmons (the second large peaks), so that the refocused microwave backscattered from target was susceptible to the nearby bright spots when the focal point is scanned. Thin lens may not be a good choice for the focus-scanning detection even if we do not consider the requirement of large detection depth.

Different from the situation of lens-fixed scanning, thin lens of $d = 0.5\lambda$ generates high resolution for the lens-combined scanning. In the lens-combined probe, the length of LHM slab is selected shorter than $L = 2\lambda$, thus the nearby surface plasmons effects are dispelled to some extent. For thin lens of $d = 0.5\lambda$, the influence of length on the surface plasmons effects is shown in Fig. 11. Different distributions of bright spots can be observed for LHM lens of different lengths. Among the three results, the one with $L = 2.0\lambda$ suffers the most influence of bright spots than the other two with $L = 0.5\lambda$ and $L = 1.0\lambda$. During the scanning, the nearby plasmons will affect the detection. That's why the system with lens-combined probe of $d = 0.5\lambda$ and $L = 2\lambda$ achieves the lowest resolution as shown in Table 1. If compared to Fig. 3(a) or Fig. 10(a), weaker nearby surface plasmons effects was observed in Figs. 11(a) and (b), therefore the lens-combined scanning with lens of $d = 0.5\lambda$ and $L = 0.5\lambda$ or $L = 1.0\lambda$ provides better resolution than the lens-fixed scanning with lens of $d = 0.5\lambda$ and $L = 20\lambda$.

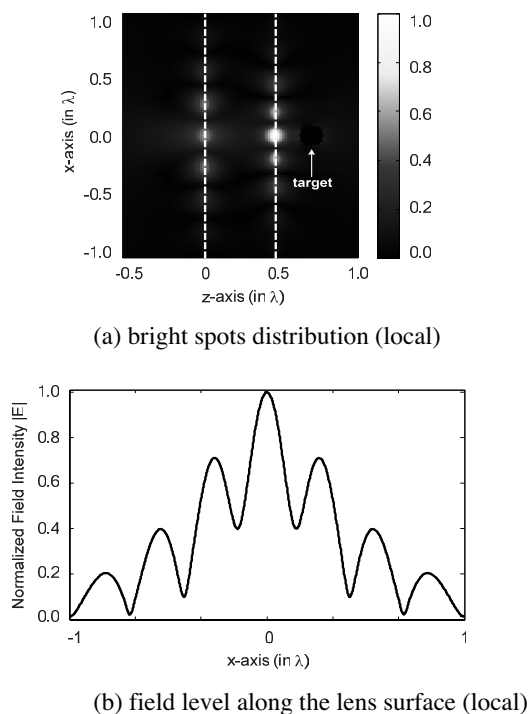


Figure 10. Plasmons effects in refocusing of backscattered microwave for LHM lens of $d = 0.5\lambda$ and $L = 20\lambda$. (a) Bright spots distribution (local). (b) Field level along the lens surface (local).

4.2. Short or Long LHM Lens

For lens-fixed scanning, longer LHM lens will benefit the detection since longer LHM will focus more energy on target and suffer less edge effects such as edge diffraction. For illustration, Fig. 12 shows the focusing of microwave backscattered from a PEC cylinder of diameter of 2 mm when the 2λ -thick LHM lens of different lengths is applied. The microwave point source is set one wavelength before the LHM lens (on the source plane), and the PEC target is set one wavelength behind the LHM lens (on the image plane). In Fig. 12, the target position is marked by a dark point and the LHM lens of thickness of 2λ is marked by white rectangular.

Figure 13 shows the corresponding lateral beam profiles of field level of refocused microwave extracted on the source plane in Fig. 12. By measuring the full width at half-maximum (FWHM) or the half-power beamwidth of the beam profiles, the variation of lateral

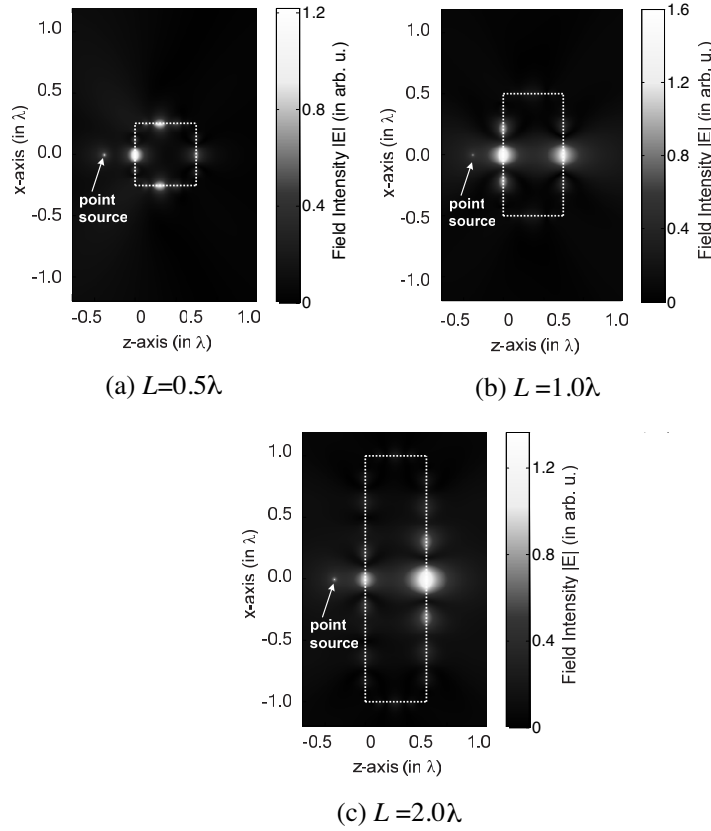


Figure 11. Different plasmons effects for LHM lens of $d = 0.5\lambda$ and different lengths L .

refocusing resolution with length of LHM lens is shown in Fig. 14.

From Fig. 14, we have the observation that the longer the LHM lens is, the better the backscattered microwave refocuses. As a result, higher imaging resolution will be achieved in the lens-fixed scanning detection.

But for lens-combined scanning, the situation becomes more complicated. From Table 1, it is observed that the thin lens of $d = 0.5\lambda$ may generate high resolution for the lens-combined scanning if the length of lens is properly selected. Considering the requirement that the lens-combined probe should be small as possible, the length should be small as possible. More simulations indicate that for length restricted within $L = 5\lambda$, shape factor $d/L = 1/2$ may be considered as guidelines for lens-combined probe design.

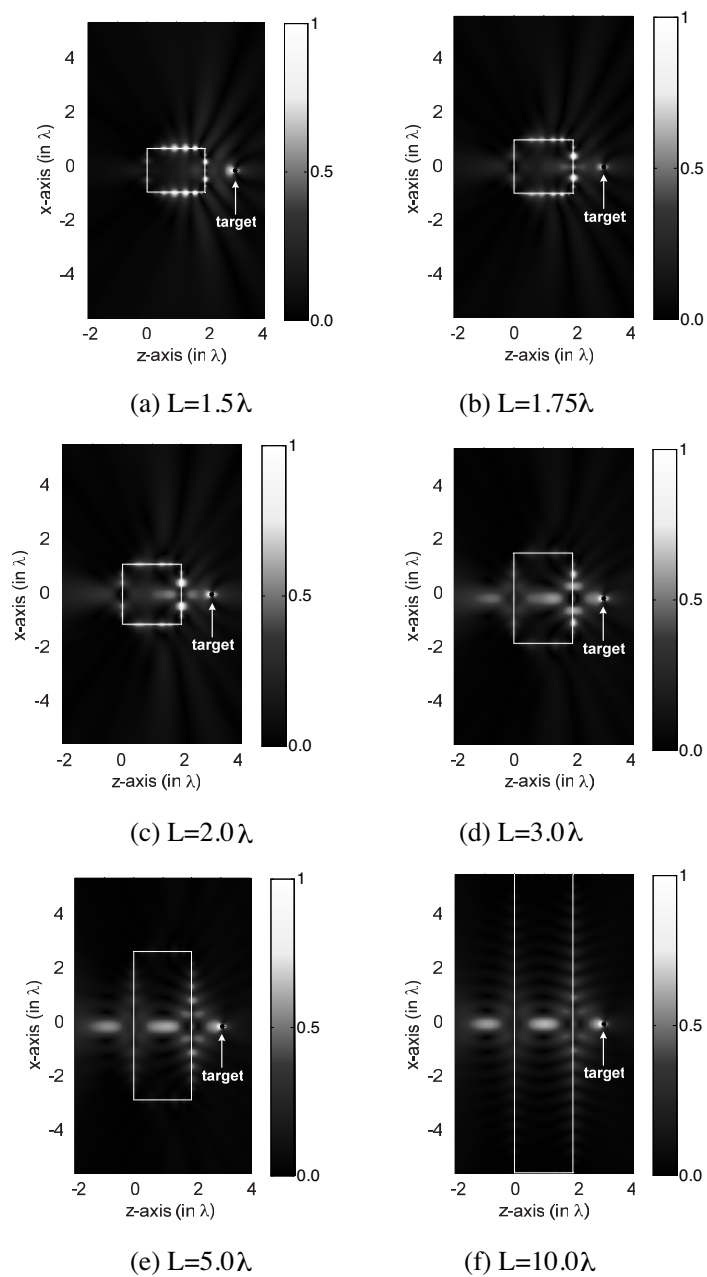


Figure 12. Refocusing of backscattered microwave when LHM lenses of $d = 2\lambda$ and different length L are used.

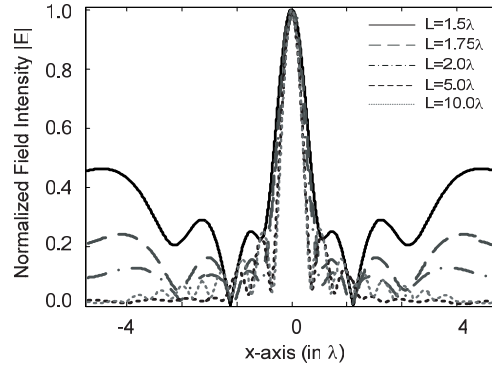


Figure 13. Lateral beam profiles of refocused microwave recorded on the source plane.

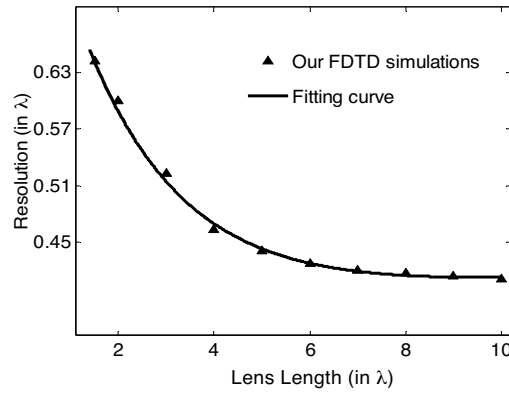


Figure 14. Lateral refocusing resolution *vs.* length of LHM lens.

4.3. Lens-fixed or Lens-combined Scanning

It is interesting to make a comparison between the lens-fixed scanning and lens-combined scanning. In the comparison, we fix the lens thickness $d = 2\lambda$.

Figure 15 shows the lateral beam profiles extracted at target position on the image reconstructed by the lens-fixed scanning scheme with LHM lens of thickness $d = 2.0\lambda$ and different L . The lateral imaging resolutions of lens of $L = 1.0\lambda$, $L = 1.5\lambda$, and $L = 2.0\lambda$ are measured to be approximately 0.46λ , 0.49λ and 0.48λ , respectively. For lens of $L = 0.5\lambda$, the imaging resolution is not measured. The lateral imaging resolution of the lens-combined scanning scheme by

using LHM lens of thickness $d = 2.0\lambda$ and different L has been shown in Fig. 9. Comparison of the two scanning approaches is given in Table 2.

From Table 2, we have the observation that for short lens, the lens-combined scanning scheme seems to provide higher resolutions than the lens-fixed scanning scheme. But the resolution is restricted to approximately 0.4λ . To acquire higher resolution, longer lens should be used. In this instance, the lens-combined probe becomes awkward and the lens-fixed scheme becomes more effective.

Table 2. Comparison of the two scanning approaches.

Resolution (in λ)	$L = 0.5\lambda$	$L = 1\lambda$	$L = 1.5\lambda$	$L = 2\lambda$
Lens-fixed scanning	—	0.46	0.49	0.48
Lens-combined scanning	—	0.38	0.43	0.46

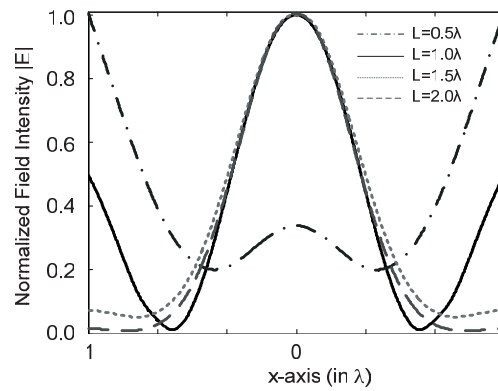


Figure 15. Lateral beam profiles extracted at target position on the image reconstructed by the lens-fixed scanning with lens of $d = 2.0\lambda$ and different L .

5. CONCLUSIONS

Some guide rules on LHM flat lens size are provided for high resolution near-field target detection and imaging by using flat LHM lens. According to different requirements on imaging resolution and data acquisition, two different approaches, *viz.* the lens-fixed scanning

and the lens-combined scanning, can be implemented. The lens-fixed scanning allows using large lens, while the lens-combined scanning approach tends to use small lens. Both the two approaches can achieve imaging resolution better than 0.4λ .

The selection of flat LHM lens size only provides a guide rule for future LHM lens design and building for near-field target detection system. More challenges lie in the realization of homogeneous and isotropic LHM.

ACKNOWLEDGMENT

This work is supported in part by Nature Science Foundation of China under Grant 60771041, Department of Personnel of Jiangsu Province of China under Grant 06-E-40, and Department of Education Jiangsu Province of China under Grant 05KJB510012.

REFERENCES

1. Veselago, V. G., "The electrodynamics of substances with simultaneously negative values of ε and μ ," *Sov. Phys. Usp.*, Vol. 10, No. 4, 509–514, 1968.
2. Caloz, C. and T. Itoh, "Metamaterials for high-frequency electronics," *Proc. IEEE*, Vol. 93, No. 10, 1744–1751, 2005.
3. Engheta, N. and R. W. Ziolkowski, "A positive future for double-negative metamaterials," *IEEE Trans. Microwave Theory Tech.*, Vol. 53, No. 4, 1535–1556, 2005.
4. Grzegorzcyk, T. M. and J. A. Kong, "Review of left-handed metamaterials: Evolution from theoretical and numerical studies to potential applications," *Journal of Electromagnetic Waves and Applications*, Vol. 20, No. 14, 2053–2064, 2006.
5. Pendry, J. B., "Negative refraction makes a perfect lens," *Phys. Rev. Lett.*, Vol. 85, 3966–3969, 2000.
6. Cummer, S. A., "Simulated causal subwavelength focusing by a negative refractive index slab," *Appl. Phys. Lett.*, Vol. 82, 1503–1505, 2003.
7. Rao, X. S. and C. K. Ong, "Subwavelength imaging by a left-handed material superlens," *Phys. Rev. E*, Vol. 68, 0676011-3, 2003.
8. Fang, N. and X. Zhang, "Imaging properties of a metamaterial superlens," *Appl. Phys. Lett.*, Vol. 82, 161–163, 2003.
9. Feise, M. W. and Y. S. Kivshar, "Sub-wavelength imaging with a

- left-handed material flat lens,” *Phys. Lett. A*, Vol. 334, 326–330, 2005.
10. Yu, G. X. and T. J. Cui, “Imaging and localization properties of LHM superlens excited by 3D horizontal electric dipoles,” *Journal of Electromagnetic Waves and Applications*, Vol. 21, No. 1, 35–46, 2007.
 11. Lagarkov, A. N. and V. N. Kissel, “Near-perfect imaging in a focusing system based on a left-handed-material plate,” *Phys. Rev. Lett.*, Vol. 92, 774011-4, 2004.
 12. Parimi, P., W. T. Lu, P. Vodo, and S. Sridhar, “Imaging by flat lens using negative refraction,” *Nature*, Vol. 426, 404, 2003.
 13. Grbic, A. and G. V. Eleftheriades, “Overcoming the diffraction limit with a planar left-handed transmission-line lens,” *Phys. Rev. Lett.*, Vol. 92, 1174031-4, 2004.
 14. Ran, L. X., J. Huangfu, H. Chen, X. M. Zhang, K.-S. Cheng, T. M. Grzegorzczuk, and J. A. Kong, “Experimental study on several left-handed metamaterials,” *Progress In Electromagnetics Research*, PIER 51, 249–279, 2005.
 15. Aydin, K., I. Bulu, and E. Ozbay, “Focusing of electromagnetic waves by a left-handed metamaterial flat lens,” *Opt. Express*, Vol. 13, 8753–8759, 2005.
 16. Wang, G., J. Fang, and X. T. Dong, “Resolution of near-field target detection and imaging by using flat LHM lens,” *IEEE Trans. Antennas Propagat.*, Vol. 55, No. 12, 3534–3541, 2007.
 17. Wang, G., J. Fang, and X. T. Dong, “Refocusing of backscattered microwaves in target detection by using LHM flat lens,” *Opt. Express*, Vol. 15, No. 6, 3312–3317, 2007.
 18. Chen, L., S. He, and L. Shen, “Finite-size effects of a left-handed material slab on the image quality,” *Phys. Rev. Lett.*, Vol. 92, No. 10, 107404-1-4, 2004.
 19. Chen, J. J., T. M. Grzegorzczuk, B.-I. Wu, and J. A. Kong, “Imaging properties of finite-size left-handed material slabs,” *Phys. Rev. E*, Vol. 74, 046615, 2006.
 20. Kissel, V. N. and A. N. Lagarkov, “Superresolution in left-handed composite structures: From homogenization to a detailed electrodynamic description,” *Phys. Rev. B*, Vol. 72, 085111, 2005.